Biochemistry

 Volume 36, Number 21 May 27, 1997

Accelerated Publications

Evolution of Lipidic Structures during Model Membrane Fusion and the Relation of This Process to Cell Membrane Fusion†

JinKeun Lee and Barry R. Lentz*

Department of Biochemistry & Biophysics, University of North Carolina, Chapel Hill, North Carolina 27599-7260

Received February 21, 1997; Revised Manuscript Received April 14, 1997⊗

ABSTRACT: The sequence of events involved in poly(ethylene glycol)-mediated fusion of small unilamellar vesicles (SUVs) has been studied. Fusion events were monitored using light scattering for vesicle aggregation, the fluorescence lifetime of membrane probe lipids (DPHpPC and NBD-PS) for membrane mixing, the aqueous fluorescent marker (Tb^{3+}/DPA and H^+/HPTS) for contents mixing; and quasi-elastic light scattering for the change in the size of vesicles. Poly(ethylene glycol) is a highly hydrated polymer that can bring vesicle membranes to near molecular contact but is unable to induce vesicle fusion without manipulations that reduce packing density and encourage molecular motions in the backbone regions of both contacting membrane leaflets. Once this condition is achieved, the sequence of events involved in vesicle fusion is shown here to be (1) outer leaflet mixing accompanied by (2) transient pore formation, both occurring on a time scale of ~10 s and leading to an initial, reversible intermediate; (3) a 1−3 min delay leading to formation of a fusion-committed second intermediate; (4) inner leaflet mixing on a time scale of *ca.* 150 s; and (5) contents mixing on a time scale of 150−300 s. Inner leaflet mixing, which has never before been shown to be distinct from outer leaflet mixing, begins simultaneously with, but is completed before, contents mixing. Fusion products, which seem to be large vesicles, are estimated to be formed from four to six SUVs. The fusion intermediates are shown to have merged outer leaflets and distinct inner leaflets prior to formation of fusion pores. Using quasi-elastic light scattering, the initial intermediate was shown to revert to SUVs upon removal of PEG, while the second intermediate irreversibly continued to a fusion pore in the presence or absence of PEG. The sequence of events for this pure lipid bilayer fusion process shows remarkable homology to what is known about the sequence of protein-mediated cell membrane fusion events, suggesting a commonality between these two processes.

Membrane fusion is a critical cellular event that connects two aqueous compartments, each surrounded by a membrane. Consequently, it must involve mixing of membrane components as well as mixing of compartment aqueous contents. Poly(ethylene glycol) (PEG[1])-mediated phosphatidylcholine vesicle fusion is a simple model (no protein, no solvent, and

† Supported by USPHS Grant GM32707.

* To whom reprint requests should be directed.

⊗ Abstract published in *Advance ACS Abstracts,* May 15, 1997.

[1] Abbreviations: ANTS, 8-aminonaphthalene-1,3,6-trisulfonic acid, disodium salt; $C_{12}E_8$, dodecyloctaethylene glycol monoether; cholic acid, 3α,7α,12α-trihydroxy-5β-cholan-24-oic acid; $DC_{18:3}PC$, 1,2-dilinolenoyl-*sn*-phosphatidylcholine; DOPC, 1,2-dioleoyl-3-*sn*-phosphatidylcholine; DPA, pyridine-2,6-dicarboxylic acid; DPX: *N,N′-p*-xylylenebis(pyridinium bromide); DPHpPC, 1-palmitoyl-2-[2-4-(phenyl-*trans*-1,3,5-hexatrienyl)phenylethyloxylcarbonyl]-3-*sn*-phosphatidylcholine; HA, hemagglutinin; HPTS, 8-hydroxypyrene-1,3,6-trisulfonic acid, trisodium salt; LUVs, large, unilamellar vesicles made by the extrusion method; NBD-PS, *N*-(7-nitro-2,1,3-benzoxadiazol-4-yl)-1,2-dioleoyl-3-*sn*-phosphatidylserine; PEG, poly(ethylene glycol); QELS, quasi-elastic light scattering; SG, secretory granules; SUVs, small, unilamellar vesicles made by sonication; TES, *N*-[tris(hydroxymethyl)-methyl]-2-aminoethane sulfonic acid.

S0006-2960(97)00404-2 CCC: $14.00

no ionic complexes) for more complicated biomembrane fusion processes. PEG can force very close contact between vesicle membranes by lowering the activity of water adjacent to the membrane (Arnold *et al*., 1990; Burgess *et al*., 1992). However, even when the vesicles are aggregated in the presence of high concentrations of PEG, no fusion is observed between large unilamellar vesicles (LUVs) composed of a single phosphatidylcholine species (Burgess *et al*., 1991a, 1992; Lentz *et al*., 1992). PEG-mediated vesicle fusion occurs only when bilayers are somehow perturbed. Fusogenic perturbation has been shown to result from high bilayer curvature (Suurkuusk *et al*., 1976; Lentz *et al*., 1987, 1992); acyl chain unsaturation within fusion-prone small, unilamellar vesicles (SUVs) (Talbot *et al*., 1997); very small surface mole fractions (0.5 mol %) of certain amphipaths (Lentz *et al*., 1992); and imperfect outer leaflet lipid packing (Wu *et al*., 1996; Lee & Lentz, 1997). Both apposing membranes must be perturbed in their outer leaflets, and fusion is blocked when perturbation is blocked (Lee & Lentz, 1997). These results emphasize the importance of imperfect lipid packing in the contacting membrane leaflets as the condition necessary to drive the lipid rearrangements needed to initiate bilayer fusion.

Much of the effort to understand the molecular mechanism of membrane fusion is aimed at determining the nature of fusion intermediates. "Hemifusion" has been reported as a fusion intermediate for model membrane (Chernomordik *et al*., 1987; Ellens *et al*., 1986; Perin & MacDonald, 1989) as well as biomembrane (Melikyan *et al*., 1995) systems. Hemifusion has been defined experimentally as mixing of lipid layers without mixing of trapped aqueous contents. Hemifusion is predicted by the "stalk−pore" mechanistic model (Chernomordik *et al*., 1987) to involve intermixing of lipids between contacting leaflets but not between noncontacting membrane leaflets. Despite accumulating evidence favoring the stalk−pore model, there has been no clear demonstration of such a mechanistically defined hemifusion intermediate, i.e., lipid mixing between membrane outer leaflets prior to the mixing of lipids between inner leaflets.

In this paper, we report the sequence of molecular events associated with PEG-mediated fusion of phospholipid vesicles with outer leaflets perturbed by a combination of high curvature and chain unsaturation (Talbot *et al*., 1997). We used light scattering to monitor vesicle aggregation driven by PEG, fluorescence lifetimes of DPHpPC (Burgess & Lentz, 1993; Wu & Lentz, 1994) and NBD-PS to monitor outer leaflet and inner leaflet lipid mixing separately, Tb^{3+}/DPA complexation to monitor trapped contents mixing (Wilschut *et al*., 1980; Talbot *et al*., 1997), HPTS to monitor proton transfer between vesicles, and quasi-elastic light scattering (QELS) to follow changes in vesicle size. Most of these measurements have been performed on a subsecond time scale using a rapid mixing device designed especially for mixing highly viscous solutions. Using these diverse methods, we have been able to demonstrate two types of fusion intermediates, both of which are consistent with and add detail to the predictions of the stalk−pore model. The sequence of events observed was (1) vesicle aggregation, (2) outer leaflet mixing and transient pore formation associated with formation of a reversible intermediate (I_1), (3) a delay before formation of an irreversibly committed intermediate (I_2), and (4) inner leaflet mixing and contents mixing. The relation of these observations to what is known about the sequence of events involved in biomembrane fusion is also discussed.

EXPERIMENTAL PROCEDURES

Materials

Chloroform stock solutions of 1,2-dioleoyl-*sn*-phosphatidylcholine (DOPC), 1,2-dilinolenoyl-*sn*-phosphatidylcholine ($DC_{18:3}PC$), and *N*-(7-nitro-2-1,3-benzoxadiazol-4-yl)-1,2-dioleoyl-3-*sn*-phosphatidylserine (NBD-PS) were purchased from Avanti Polar Lipids, Inc. (Birmingham, AL) and used without further purification. The concentrations of phospholipid stocks were determined by phosphate assay (Chen *et al*., 1956). 1-Palmitoyl-2-[2-4-(phenyl-*trans*-1,3,5-hexatrienyl)phenylethyloxylcarbonyl]-3-*sn*-phosphatidylcholine (DPHpPC), 8-aminonaphthalene-1,3,6-trisulfonic acid disodium salt (ANTS), *N*,*N*′-*p*-xylylenebis(pyridinium bromide) (DPX), and 8-hydroxypyrene-1,3,6-trisulfonic acid, trisodium salt (HPTS) were purchased from Molecular Probes (Eugene, OR). Terbium (Tb^{3+}) chloride was purchased from Johnson Matthey Co. (Ward Hill, MA). Dipicolinic acid (DPA), 3α,7α,12α-trihydroxy-5β-cholan-24-oic acid (cholic acid), and *N*-[tris(hydroxymethyl)methyl]-2-aminoethane sulfonic acid (TES) were purchased from Sigma Chemical Co. (St. Louis, MO). Carbowax PEG 8000 (molecular weight of 7000−9000) was from Fisher Scientific (Fairlane, NJ) and further purified as previously described (Lentz *et al*., 1992). Sodium dithionite was from Fluka Chemical Co. (Ronkonkoma, NY). Dodecyloctaethylene glycol monoether ($C_{12}E_8$) was purchased from Calbiochem (La Jolla, CA). All other reagents were of the highest quality available.

Methods

Vesicle Preparation. Small unilamellar vesicles were prepared as described by Lentz *et al*. (1987). A mixture of DOPC and $DC_{18:3}PC$ (85/15 mol %) in chloroform was dried under nitrogen. For vesicles used in lipid mixing measurements, an appropriate mole fraction of probe lipids was added to the chloroform solution prior to drying. The dried lipids were dissolved in cyclohexane with an aliquot of methanol (about 5 vol %), frozen in dry ice, and dried under high vacuum overnight. The dried lipids were resuspended in an appropriate buffer for about 1 h at room temperature above the main phase transition. To prepare SUVs, the lipid suspension was sonicated using a Heat Systems model 350 sonicator (Plainview, NY) equipped with a titanium probe tip. Vesicle preparations were fractionated by centrifugation at 70 000 rpm for 25 min at 4 °C using a Beckman TL-100 ultracentrifuge (Palo Alto, CA). The buffers were prepared as described in Talbot *et al*. (1997) for the ANTS/DPX leakage and Tb^{3+}/DPA contents mixing assays. Buffers contained 100 mM NaCl, 1 mM EDTA, and 2 mM TES at appropriate pH's (7.4 except for the H^+/HPTS assay).

Membrane Mixing Assays. Both membrane mixing assays use the fact that the lifetime of the membrane-located probe is a sensitive function of its surface concentration in the membrane. For DPHpPC, this phenomenon has been documented and explained in the literature (Lentz & Burgess, 1989; Burgess & Lentz, 1993), while for NBD-PS, it is documented in Figure 1. SUVs composed of DOPC/$DC_{18:3}PC$ (85/15 mol %) with different lipid/probe ratios (a final lipid concentration of 0.5 mM) were monitored at 23 °C in

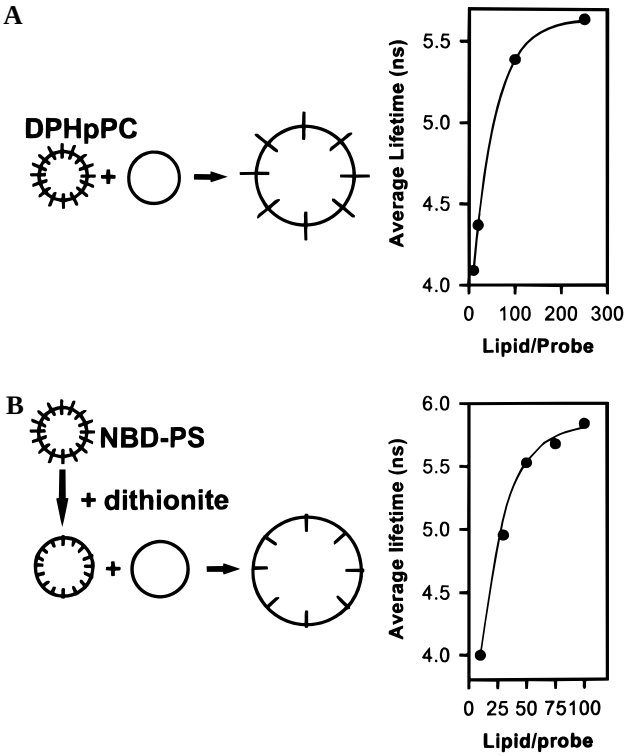

FIGURE 1: Membrane mixing assays using the fluorescence lifetime of membrane probe lipids. Fluorescence lifetimes of DPHpPC and NBD-PS increase with an increasing lipid/probe ratio. Since these membrane probes are diluted during fusion between probe-rich and probe-free vesicles, a measurable increase in their fluorescence lifetimes results. The diagrams show probe dilution during fusion, and the corresponding plots are the average lifetimes of the probe in DOPC/$DC_{18:3}$PC SUVs with different lipid/probe ratios. Solid lines were obtained as described by Burgess and Lentz (1993). (A) The dependence of the DPHpPC lifetime on the lipid/probe ratio is shown along with an illustration of the membrane mixing assay. Using this probe lipid, we were able to distinguish outer and inner leaflet mixing as two clearly separable increases in DPHpPC lifetime (Figure 2A). (B) The dependence of the lifetime of the inner leaflet NBD-PS on the lipid/probe ratio is shown along with an illustration of this inner leaflet membrane mixing assay. NBD-PS in the outer leaflet of probe-rich vesicles was reduced with dithionite to leave only the inner leaflet fluorescently labeled (Meers *et al*., 1992). This assay corroborated the interpretation of our DPHpPC results (Figure 2).

the presence of 17.5 wt % PEG. NBD-PS-labeled vesicles were treated with sodium dithionite (200/1 dithionite/NBD-PS) to reduce NBD located in their outer leaflets (McIntyre & Sleight, 1991; Meers *et al.*, 1992, 1996; Lentz *et al.*, 1997). Sodium dithionite was separated from the vesicles using a Sephadex G-75 column. In this way, observed increases in NBD lifetime must reflect inner leaflet lipid mixing associated with fusion (Figure 1).

Fluorescence measurements were made on an SLM 48000 MHF spectrofluorometer (SLM Instruments, Rochester, NY) equipped with a Coherent Inova 90 argon-ion laser (Coherent Auburn Group, Auburn, CA) using the laser UV multiline (351.1−363.8 nm) for DPHpPC and a laser line at 488 nm for NBD-PS. Emission was detected at an angle of 54.7° from the vertical through a 3 mm KV-450 filter or through a 2 mm OG-515 filter (Schott Optical Glass, Duryea, PA) for DPHpPC and NBD-PS, respectively. The Dynamic Data Acquisition routine of the SLM 48000 MHF spectroscopy software package was used to collect phase shifts and modulation ratios at 37 frequencies (with a base frequency of 4 MHz) using a 5 s acquisition time and a 300-acquisition average, and a glycogen solution as a zero-lifetime reference.

Phase-resolved lifetimes and intensity fractions of each component were estimated using the Global Analysis software package (Globals Unlimited, Urbana, IL). Average lifetimes were obtained from three lifetime-component analyses for DPHpPC (Wu & Lentz, 1994) and two lifetime-component analyses for NBD-PS. Errors in lifetime determinations were typically in the range of 0.05 ns on the basis of the uncertainty from Globals error analysis with one standard deviation confidence. The average lifetime (τ_{AV}) was calculated from

$$\tau_{AV} = \sum_i f_i \tau_i \quad (1)$$

where f_i and τ_i are the intensity fraction and lifetime of the ith component, respectively (Lakowicz, 1983).

Rapid mixing of vesicles and PEG was accomplished using a pneumatically driven stopped-flow accessory (model RX1000) from Applied Photophysics (Leatherhead, U.K.; Burgess *et al.*, 1991b). The two vesicle populations for each assay were mixed just before loading into one of two sample syringes in the stopped-flow device. The other syringe was loaded with 26.25 wt % PEG solution, and the injection port on this side was fitted with an oversized orifice (Burgess *et al.*, 1991b). Vesicles and PEG solutions were injected simultaneously to the mixing chamber with a pressure of 6 bar to a final lipid concentration of 0.5−0.6 mM and a PEG concentration of 17.5 wt %. A microswitch in the exit port triggered data collection. The temperature was maintained at 23 °C by water circulation through both the SLM 48000 MHF fluorometer chamber and the stopped-flow device. Labeled vesicles used for the DPHpPC lipid mixing assay and NBD-PS inner leaflet mixing assay were prepared with a lipid/probe of 10 as described (Burgess & Lentz, 1993; Lentz *et al*., 1997) and were mixed with 10 and 5 volumes of unlabeled vesicles for DPHpPC and NBD-PS assays, respectively. To minimize potential photolysis of the probes by the laser light, a UV-NIR beam spreader (model 15600 with input lens 15630; Oriel Instruments, Stratford, CT) was placed in the incident light beam. Phase shifts and modulation ratios were collected at 30 frequencies (with a base frequency of 4 MHz) using a 50 Hz correlation frequency, a 1 s analysis window, and a 50-acquisition average.

Contents Mixing Assays. Trapped aqueous contents mixing was monitored by two methods, the Tb^{3+}/DPA assay and a newly introduced H^+/HPTS assay. The Tb^{3+}/DPA assay monitors fluorescent complex formation between Tb^{3+} and DPA trapped in separate populations of vesicles (Wilschut *et al*., 1980). This assay was easily adapted to our rapid mixing device because it can be performed quantitatively in the presence of PEG (Viguera *et al*., 1993; Talbot *et al.*, 1997). We tested for leakage of aqueous contents due to vesicle rupture (Massenburg & Lentz, 1993) by monitoring the fluorescence of ANTS coencapsulated with its quencher DPX as described in Lentz *et al.* (1992), except that fluorescence was measured without dilution of PEG. The time course of contents leakage was obtained from the time dependence of fluorescence intensity referenced to the fluorescence observed after addition of detergent ($C_{12}E_8$) to obtain the percent leakage (Talbot *et al*., 1997). Contents mixing as a percent of that expected from complete fusion

of vesicle dimers was calculated after referencing to the fluorescence after detergent (sodium cholate) was added and correcting for the fluorescence of Tb^{3+}/DPA coencapsulated in SUVs treated with PEG (Talbot *et al*., 1997). For both assays, reference values were obtained using fluorescence cuvettes, since detergent could not be added to the rapid mixing chamber. Fluorescence intensities from the cuvette experiment were scaled to those from the rapid mixer by matching the data obtained by both methods in the range of 30−45 s. After scaling, time courses obtained by both methods were indistinguishable beyond 30 s.

The H^+/HPTS assay depends on the sensitivity of the HPTS absorption spectrum to the H^+ concentration (Clement & Gould, 1981). For our assay, one population of vesicles was prepared in a buffer containing 0.5 mM HPTS at pH 8.0. Untrapped HPTS was separated from vesicles using a Sephadex G-75 column (Pharmacia, Piscataway, NJ). The other population of vesicles was prepared without HPTS at pH 5.5, and the pH of its external compartment was adjusted to pH 8.0. These two types of vesicles were mixed in a 1/10 ratio (0.05 mM probe-containing vesicles/0.5 mM probe-free vesicles). A decrease of HPTS fluorescence indicated exposure of HPTS to an increased concentration of protons. Since the molecular mass of HPTS is 524 amu and since protons diffuse very rapidly in water solutions (Paula *et al.*, 1996), diffusion of protons from the pH 5.5 to the pH 8.0 trapped compartments is expected to be primarily responsible for a fluorescence decrease, especially for diffusion through a small pore. To detect proton leakage across SUV membranes, both probe-containing and probe-free vesicles were prepared at pH 8.0 and their external pH was adjusted to pH 5.5.

Measurements of Vesicle Aggregation and Vesicle Size. Vesicle aggregation was followed by 90° light scattering measured at a wavelength of 500 nm in the SLM 48000 MHF spectrofluorometer. Data were corrected for scattering caused by PEG alone. For vesicle size determination, quasi-elastic light scattering (QELS) measurements were carried out by methods described previously (Lentz *et al*., 1992) using a locally built multiangle instrument equipped with a Spectra-Physics Stabilite model 120 S helium−neon laser (632.8 nm) and a computer-controlled Nicomp 170 auto-correlator (Particle Sizing Systems, Inc., Santa Barbara, CA). Vesicles were added at 23 °C to 17.5 wt % PEG to a final concentration of 0.5 mM lipid. After different incubation times, vesicles were rapidly (≤2 s) diluted 20-fold and used for QELS measurements immediately (<20 s) or after further incubation at 23 °C. Control experiments showed that vesicles were not aggregated by the low PEG concentration achieved after dilution.

RESULTS

Outer Leaflet Mixing Precedes Inner Leaflet Mixing by a Delay. Lipid mixing assays using dyes such as R18 and DiI (Kemble *et al*., 1994; Zimmerberg *et al*., 1994; Hoekstra *et al*., 1984) incorporated into the cell membrane *via* a simple diffusion mechanism measure mainly outer leaflet lipid mixing. These assays suffer both from potential intermembrane transfer through the aqueous medium [e.g., see Tse *et al.* (1993) in the case of R18] and from a relative signal that is difficult to interpret quantitatively. DPHpPC and NBD-PS are fluorescent lipids that redistribute, as do most polar lipids, very slowly between and across membranes (Lentz *et al*., 1995; Meers *et al*., 1996; Wu & Lentz, 1991) and provide an intensive quantity (lifetime) that can be interpreted quantitatively in terms of probe surface concentration in both outer and inner leaflets (Wu & Lentz, 1994). The time course of membrane mixing in PEG-mediated SUV fusion is shown in Figure 2. DPHpPC is located in both membrane leaflets, and dilution of the probe must, therefore, occur in both leaflets during fusion. An increase in fluorescence lifetime of DPHpPC is a reflection of probe dilution (Burgess & Lentz, 1993), which indicates membrane mixing. The average fluorescence lifetime of DPHpPC in DOPC/$DC_{18:3}$PC SUVs in the presence of 17.5 wt % PEG as a function of time showed a biphasic increase (Figure 2A), indicating two well-separated events that contributed to membrane lipid mixing.

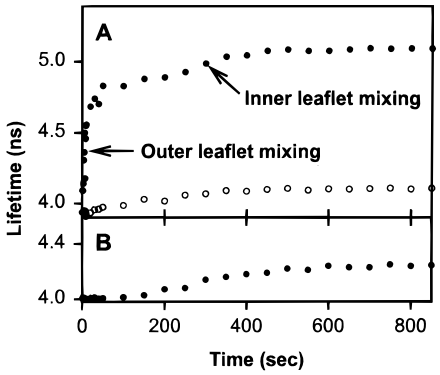

FIGURE 2: Time course of membrane mixing in PEG-mediated SUV fusion. Membrane mixing in DOPC/$DC_{18:3}$PC SUVs in the presence of 17.5 wt % PEG was monitored by the fluorescence lifetime increase of DPHpPC (A) and NBD-PS (B). PEG was added to vesicles at time zero. The fluorescence lifetime of DPHpPC showed a two-step increase, indicating two separate membrane mixing events. An increase in the lifetime of NBD-PS did not occur until some time after the first DPHpPC lifetime change had been completed and then paralleled the second increase in the DPHpPC lifetime. This clearly confirms that the first and second increase in the DPHpPC lifetime reflected outer and inner leaflet mixing, respectively, and that these events were separated by a well-defined delay. As a control experiment, membrane mixing in DOPC SUVs in the presence of 15 wt % PEG was monitored by the fluorescence lifetime increase of DPHpPC (A, open circles).

The first lipid mixing event occurred immediately after vesicle aggregation (Figure 4A), while the second started roughly 180−200 s after vesicles and PEG were mixed. Our interpretation is that the first event represents intermingling of lipids between the outer leaflets of hemifused membranes, while the second represents mixing of lipids between the inner leaflets of fully fused membranes. In order to test this interpretation, we used an assay specific for inner leaflet mixing. Figure 2B shows the time dependence of the fluorescence lifetime of NBD-PS located in inner leaflets of the same vesicle system (see Methods and Figure 1) and demonstrates that inner leaflet lipid mixing started roughly 180 s after vesicles and PEG were mixed. We show elsewhere that the distribution of NBD-PS in these vesicles remained unperturbed by the fusion process (Lentz *et al.*, 1997). This indicates that the second step increase in the DPHpPC lifetime is mainly due to inner leaflet mixing. The half-time of outer leaflet mixing (<10 s) was much shorter than that of inner leaflet mixing (∼150 s). Due both to the lower lipid content of the SUVs' inner leaflets (42% of total mass) and to the intensity-weighted fashion in which

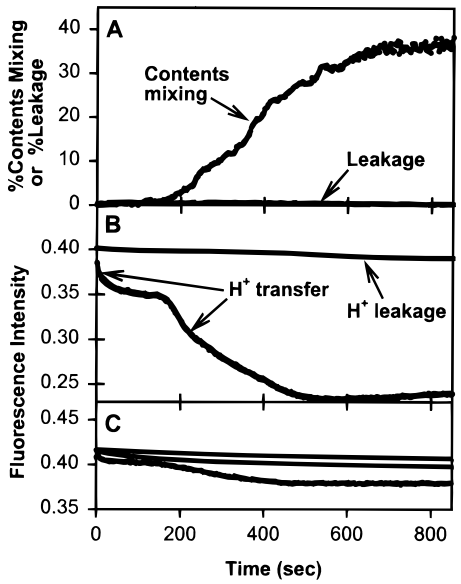

FIGURE 3: Time course of aqueous contents mixing in PEG-mediated SUV fusion. Mixing of trapped aqueous contents in DOPC/$DC_{18:3}$PC SUVs in the presence of 17.5 wt % PEG was monitored by Tb^{3+}/DPA complexation (A) and proton transfer (B). Proton transfer was monitored by a decrease in fluorescence intensity of HPTS; this was biphasic, with initial transfer occurring simultaneously with outer leaflet mixing (Figure 2). The second phase of proton transfer (frame B), Tb^{3+}/DPA complexation (frame A), and inner leaflet mixing (Figure 2) started nearly simultaneously. No noticeable leakage was observed by the ANTS/DPX assay (A), while a small but detectable proton leakage was observed (B). As control experiments, proton leakage (C, top) and proton transfer (C, middle) for DOPC SUVs in the presence of 15 wt % PEG, as well as proton transfer (C, bottom) for DOPC SUVs in the presence of 17.5 wt % PEG, were monitored.

fluorescence lifetimes average (eq 1; Wu & Lentz, 1994), the increase in the average DPHpPC lifetime associated with inner leaflet mixing was much smaller than that associated with outer leaflet mixing.

As a control, the lifetime of DPHpPC in DOPC SUVs in the presence of 15 wt % PEG is shown in Figure 2A (open circles). This lipid system showed no sign of vesicle contents mixing under these conditions (Talbot *et al.*, 1997; Figure 3C). The lifetime increase observed was much smaller and occurred much more slowly than that observed for DOPC/$DC_{18:3}$PC SUVs in the presence of 17.5 wt % PEG. We presume that this results from slow lipid transfer between the outer leaflets of aggregated but unfused vesicles (Wu & Lentz, 1991; Burgess *et al.*, 1991b). Thus, the substantial biphasic increase in DPHpPC lifetime was due to sequential merging, first of outer leaflets and then of inner leaflets. We have shown previously that the observed average lifetime associated with the mixing of outer leaflets of aggregated vesicles can yield an estimate of the most likely aggregate size (Wu & Lentz, 1994). Using this analysis, we estimated from the lifetime following outer leaflet mixing (~4.8 ns) that four or five SUVs are involved in forming a single aggregate. Using a similar approach based on the assumption of complete fusion (mixing of both inner and outer leaflets), we estimated from the final limiting lifetime (~5.1 ns) that five or six SUVs participate in forming the final fusion product.

Trapped Aqueous Contents Mixing and Inner Leaflet Mixing Start Simultaneously. The time course of aqueous contents mixing in PEG-mediated SUV fusion is shown in Figure 3. Mixing of Tb^{3+} and DPA trapped separately in DOPC/$DC_{18:3}$PC SUVs in the presence of 17.5 wt % PEG was delayed by approximately 180 s from the time when vesicles and PEG were mixed (Figure 3A, circles) but began simultaneously with inner leaflet mixing (Figure 2). Contents mixing, however, was slower ($t_{1/2} \sim 200-300$ s) than inner leaflet mixing ($t_{1/2} \sim 150$ s). No noticeable leakage was observed in this particular vesicle system during the entire fusion process (Figure 3A, squares), in agreement with earlier end point measurements (Lentz *et al.*, 1997).

A Transient Proton Pore Is Associated with Outer Leaflet Mixing. The time course of the fluorescence change due to HPTS trapped in one vesicle population being exposed to H^+ trapped in a second vesicle population is shown in Figure 3B (circles). Proton leakage to the extravesicular compartment was barely detectable (Figure 3B) and, even if it did occur, could not contribute to our observations because of the way in which our proton transfer assay was designed. The decrease in HPTS fluorescence was biphasic; a fast initial transfer was followed by a slow transfer (Figure 3B). Proton transfer occurred immediately after vesicle aggregation with a time course similar to that of outer leaflet mixing. This H^+ transfer is suggested to be due to transient pore formation (see Discussion). The major fluorescence change occurred in the second phase, whose time course paralleled that of inner leaflet mixing. We suggest that second phase proton transfer reflects contents mixing *via* fusion pore formation, although proton transfer was somewhat faster ($t_{1/2} \sim 150$ s) than Tb^{3+}/DPA mixing ($t_{1/2} \sim 200-300$ s).

In control experiments, we tested vesicle systems for which contents mixing is not detected by a single-point determination using the Tb^{3+}/DPA assay. DOPC SUVs at 15 wt % PEG (Figure 3C, middle curve) and 17.5 wt % (Figure 3C, bottom curve) both showed a small amount of proton transfer but no Tb^{3+}/DPA single-point contents mixing (Talbot *et al.*, 1997). Apparently, the time course of proton transfer provides a much more sensitive measure of intervesicle pore formation than does the Tb^{3+}/DPA assay. Indeed, a very small amount of fusion (indicated by a biphasic HPTS fluorescence time course; see Discussion) was detectable for DOPC SUVs at 17.5 wt % PEG in the H^+ transfer assay, even though the Tb^{3+}/DPA assay detects no fusion (Talbot *et al.*, 1997).

Reversible and Irreversible Intermediates Are Involved in the Fusion Process. Vesicle aggregation began immediately after the vesicles were mixed with 17.5 wt % PEG and was completed within 200 ms (Figure 4A). Thus, aggregation was completed well before any other fusion events occurred. Using QELS, we were able to obtain estimates of the vesicle or aggregate diameters by diluting the PEG-aggregated samples at various times throughout the fusion process (Figure 4B, filled circles). The particle diameter determined immediately (≤2 s) after addition of PEG to DOPC/$DC_{18:3}$PC SUVs was indistinguishable from that determined prior to PEG addition (~450 Å), indicating that aggregation was completely reversible. Surprisingly, a sample diluted 50 s after vesicles and PEG were mixed, well after outer leaflets had mixed, contained particles of the same mean diameter and distribution width (Figure 4B). Thus, dilution of PEG disassembled the initial aggregates before or after outer leaflet mixing had occurred. Large increases in both particle diameters and diameter distribution widths (vertical bars in Figure 4B) were observed only later in the

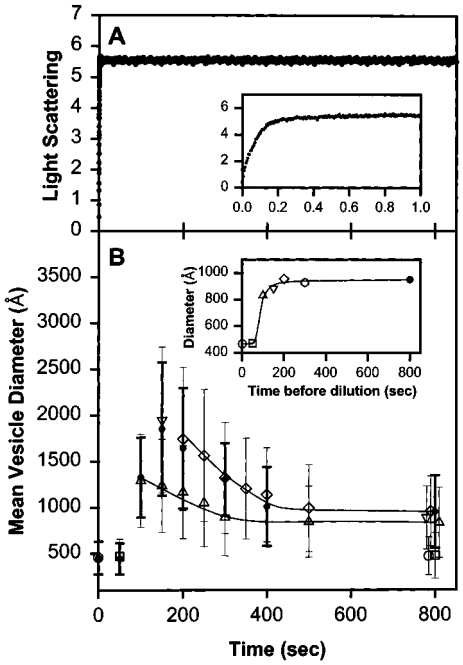

FIGURE 4: Vesicle aggregation and vesicle size during the fusion process. (A) Vesicle aggregation driven by 17.5 wt % PEG was monitored by 90° light scattering recorded at 500 nm. The inset shows the time course of light scattering for 1 s after PEG addition. Time zero was set as the time that vesicles and PEG reached the cuvette and mixed (determined to be 60 ms after plunger activation). (B) The mean particle diameter and Gaussian distribution width (vertical bars) were determined by QELS after removal of PEG at various times during the fusion process. Data were obtained immediately after removing PEG from samples incubated at 23 °C in PEG for the indicated times (filled circles). In experiments reported as open symbols, SUVs were incubated for 0 (circles), 50 (squares), 100 (triangles), 150 (inverted triangles), 200 (diamonds), and 300 s (hexagons) prior to dilution of PEG and then further incubated up to the total time indicated (after original PEG addition) before recording QELS data. The inset shows the final diameter of the fusion product from these experiments (determined 800 s after PEG was initially added) as a function of the time at which PEG was diluted.

fusion process. These increases occurred during the delay between the completion of outer leaflet mixing and the initiation of inner leaflet mixing (Figure 4B). During the time course of inner leaflet mixing (roughly 200−450 s), the average particle diameter decreased to a limiting value of 950 Å. Assuming that this final product of the fusion process was a unilamellar vesicle with a surface area equal to the sum of the surface areas of the SUVs that fused to form it, we estimate that an average of four and one-half SUVs fused during this PEG-mediated fusion process. Since we estimated from the DPHpPC average lifetime that four to six SUVs were aggregated and fused in the presence of PEG, it seems that nearly all the vesicles in an aggregate fused to form a unilamellar product during the course of fusion in the presence of PEG. Given this estimate of the size of the fusing complex, it seems most likely that the complex consists of a trigonal bipyramid of contacting SUVs.

These particle diameter data imply that at least two types of intermediate structures form during the fusion process. The first intermediate (I_1), having intermingled outer leaflets and small pores that allow the passage of H^+, reverts to SUVs upon removal of PEG. The increase in the apparent aggregate size, which begins between 50 and 100 s and continues until 150−200 s after aggregation, indicates the formation of another structure. About 200 s after aggregation, this structure seems to begin to decay to the final fusion product, with a decay time that is the same as that observed for formation of the second H^+ pore (Figure 3B) and mixing of inner leaflet lipids (Figure 2). These observations strongly indicate this second structure as the second fusion intermediate (I_2), which apparently is stable with regard to PEG dilution. To test whether this structure represents an intermediate necessary and sufficient for formation of the final fusion product, we performed experiments in which we arrested the normal time course of the fusion process by dilution of PEG at various times and then incubated for different times before determining apparent particle diameters. As long as SUVs were incubated for 200 s with 17.5 wt % PEG before dilution, the fusion process proceeded to completion with exactly the same time course in the presence or absence of PEG (compare filled circles to open diamonds in Figure 4B). However, if the fusion process was interrupted by dilution 100 s after aggregation, fusion proceeded with a similar time course, but to a smaller final product (open triangles in Figure 4B). Arresting the process at several different times followed by incubation until 800 s demonstrated a clear correlation between the final product mean diameter and the time of dilution (inset to Figure 4B). These data strongly support the hypothesis that formation of a second intermediate structure (I_2) is necessary and sufficient for completion of the fusion process.

DISCUSSION

Sequential Model for PEG-Mediated Vesicle Fusion. The data presented here provide a detailed picture of the sequence of events leading to fusion of model lipid bilayers held in close contact by PEG, as summarized in Figure 5. PEG-mediated vesicle fusion began with vesicle aggregation which was completed before outer leaflet mixing began. Burgess *et al.* (1991b) reported that the rate of intermembrane lipid transfer was enhanced in vesicles aggregated by 17.5 wt % PEG, but not nearly to the extent observed here for vesicles that fused at this same PEG concentration. This rapid intermembrane transfer in a fusing system presumably depends on the disrupted outer leaflet packing that we have demonstrated is necessary for fusion (Wu *et al.*, 1996; Lee & Lentz, 1997; Talbot *et al.*, 1997). In the model membranes studies here, outer leaflet disruption is derived from a combination of high curvature and chain unsaturation (Talbot *et al.*, 1997). This very rapid lipid mixing between contacting, destabilized outer leaflets is interpreted as signaling formation of an initial prefusion intermediate (I_1), with a lipidic connection between contacting membrane leaflets (Figure 5, second down from top left). This is the first sign during the fusion process of the formation of a hemifusion state, defined mechanistically in terms of joining of contacting outer leaflets without intermingling of inner membrane leaflets (Chernomordik *et al.*, 1995). Hemifusion has been reported experimentally in terms of lipid mixing without pore formation (Kemble *et al.*, 1994), but the data in Figure 2, we believe, provide the first direct proof that mixing of outer leaflet components during membrane fusion is observed as an event kinetically separate from inner leaflet mixing and, thus, that the mechanistically defined hemifused state exists.

During formation of the I_1 state, fast intervesicle proton transfer occurred with a time course nearly identical to that of outer leaflet mixing but ceased well before proton transfer

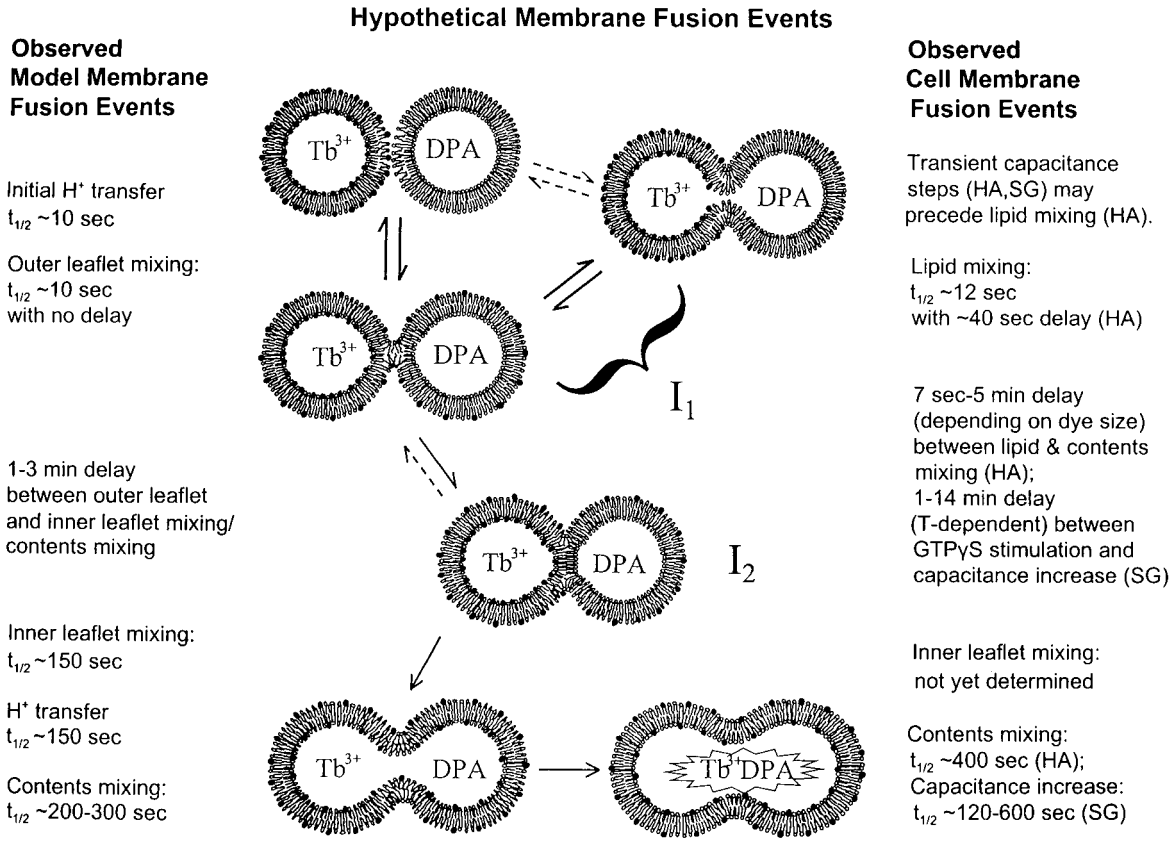

FIGURE 5: Proposed sequence of events leading to lipid vesicle and biomembrane fusion. Time scales of model membrane events are based on results presented here. Vesicles are rapidly aggregated by PEG treatment (top left). Disrupted outer leaflet packing initiates the fusion process. The first step begins with outer leaflet lipid mixing between two contacting outer leaflets which forms intermediate I_1 (second down from top left). This is proposed to be a dynamic mixture of the stalk suggested by Koslov *et al*. (1989) and a transient pore. This unstable intermediate reverts to SUVs when PEG is diluted and appears to reversibly relax to transient pores in the presence of aggregating concentrations of PEG (top right). If membrane contact is maintained, I_1 can mature to develop a semistable intermediate (I_2) separating two aqueous compartments (third down from top left). This is proposed to be the single-bilayer septum also discussed by Koslov *et al*. (1989). Disintegration of I_2 forms an irreversible pore (bottom left). Dilation of the pore allows mixing of aqueous contents and completes the fusion process (bottom right). Time scales of cell membrane fusion events are from kinetic studies of fusion either between red blood cells and hemagglutinin-expressing fibroblasts (HA) (Zimmerberg *et al*., 1994) or between mast cell plasma membrane and secretory granules (SG) (Fernandez *et al.*, 1984; Spruce *et al.*, 1990; Oberhauser *et al*., 1992).

had ended (Figure 3B). For this reason, we suggest that this initial proton transfer is due to flickering pores that occur during the transient I_1 state. The instability of the I_1 state was demonstrated by our observation that it reverted to SUVs after dilution of PEG (Figure 4B). The properties of the I_1 state lead us to suggest in Figure 5 that it may consist of a dynamic mixture of the hypothetical stalk structure proposed by Kozlov *et al.* (1989) and a transient pore. Melikyan *et al*. (1995) studied hemifusion between planar bilayer membranes and cells expressing a mutant hemagglutinin (HA) linked to the membrane by a lipid. These authors observed lipid mixing in the absence either of a flickering pore or of a subsequent fusion pore. We have observed initial proton transfer only in systems that proceed to fusion pores. It may be that lipid-linked HA produces a structure different from the hemifusion intermediate structure that is produced during the normal fusion process, thus accounting for the absence of transient pores in the work of Melikyan *et al.* (1995).

If SUVs remained aggregated by PEG, the principal fate of the I_1 state was evolution to a semistable intermediate (I_2) that ultimately decayed irreversibly to a fusion pore. Our measurements of aggregate size (Figure 4B) clearly documented the formation, at times beyond 50 s, of a semistable structure that, by 100−200 s, had begun to transform into fusion product, even in the absence of PEG. Also consistent with the formation of a structure different from I_1, the rate of intervesicle proton transfer slowed during this same time period. The long delay between formation of the I_1 and I_2 states (100−150 s) suggests that significant molecular rearrangements are needed for maturation of the initial to the final prefusion intermediate. The slight increase in DPHpPC and NBD-PS lifetimes around 150 s (Figure 2) suggests that these rearrangements dilute slightly the high surface concentration of probe on the inner leaflet. The I_2 state formed by this molecular rearrangement is presumed in Figure 5 to be the "single-bilayer septum" proposed as a possible intermediate by Kozlov *et al.* (1989). Formation of the septum structure from the stalk structure requires the movement of lipid from the outer to the inner membrane leaflet, which could explain why the process is slow and why the lifetime of inner leaflet-located probe increased slightly from 50 to 200 s. We show elsewhere that PEG-mediated vesicle fusion causes transmembrane lipid movement from the outer to the inner leaflet, but not from the inner to the outer leaflet (Lentz *et al*., 1997). Interestingly, no such delay was observed between lipid mixing and contents mixing in Ca^{2+}-induced fusion of phosphatidylserine vesicles (Wilshut & Hoekstra, 1986), suggesting that the lipid rearrangements involved in this process may not be the same as those involved in either PEG-mediated fusion or biomem-

brane fusion.

Fusion pore formation was detected by the nearly simultaneous initiation of inner leaflet mixing and contents mixing (Figures 2 and 3A) and the resumption and completion of proton transfer (Figure 3B). We propose that irreversible disintegration of the I_2 intermediate leads to fusion pore formation. This irreversible process may be a consequence of septum growth, which should cause continued stress to the junction as the unstable annulus around the septum grows. We note that Tb^{3+}/DPA mixing was slower ($t_{1/2} \sim 200-300$ s) than either H^+ transfer ($t_{1/2} \sim 150$ s) or inner leaflet lipid mixing ($t_{1/2} \sim 150$ s). This could reflect slower diffusion through the small aqueous pore than through the lipid bilayer due to slow dilation of fusion pores (Chizmadzhev *et al*., 1995). Measurements with different sized aqueous markers will be needed to test for pore dilation.

PEG-Mediated Vesicle Fusion Parallels Protein-Mediated Biomembrane Fusion. Finally, we point out that there are remarkable similarities between the course of events that we have defined here for PEG-mediated SUV fusion and the sequence of events defined in the literature for fusion of biomembrane systems (see Figure 5). To begin with, electrophysiological measurements of cellular membrane fusion have suggested the formation of transient or flickering pores (Figure 5, top right) in the early stages of secretory granule (SG)- or hemagglutinin (HA)-mediated cell fusion (Fernandez *et al.*, 1984; Breckenridge & Almers, 1987; Spruce *et al*., 1990, 1991; Zimmerberg *et al.*, 1994). These observations led to the proposal that the early events in fusion of biomembrane systems were reversible, as opposed to the irreversible events occurring near the end of the fusion process (Breckenridge & Almers, 1987; Spruce *et al.*, 1990; Monck *et al.*, 1995). In the SG system, initial capacitance flickering occurs 1 min or more before an irreversible capacitance step (Fernandez *et al*., 1984; Spruce *et al.*, 1990; Oberhauser *et al.*, 1992), although there is little information about the relationship of flickering pores with spontaneous lipid mixing. However, in one report of HA fusion (Zimmerberg *et al.*, 1994), pore flickering occurred only a few seconds prior to lipid mixing. This very small lag between flickering and lipid mixing is probably due to inhibition of lipid diffusion by the protein components of the fusion complex. This represents one difference between the biomembrane and lipid membrane processes. However, in HA-mediated biomembrane fusion, there was still a lag after flickering of roughly 200 s before aqueous markers recorded a stable fusion pore. Since electrophysiological techniques cannot be used to monitor transient conductive pores between PEG-aggregated SUVs, it was not possible to test directly for such transient pores in PEG-mediated vesicle fusion. However, since protons diffuse very rapidly in water (Paula *et al.*, 1996), proton transfer measurements should mimic the conductivity measurements provided by electrophysiological techniques. For PEG-mediated fusion of pure lipid SUVs, we have observed mixing of outer leaflet lipids simultaneously with the formation of proton-permeant transient pores (Figures 2A and 3B). Just as for biomembrane fusion, this early stage of PEG-mediated SUV fusion is reversible; it is not until I_2 formation that events lead irreversibly to a true fusion pore (Figure 4).

In both biomembrane systems, flickering pores preceded fusion pore formation (marked by contents mixing or granule release) by a substantial delay. This delay between the reversible and irreversible events that occur during both biomembrane fusion processes is reminiscent of the clear delay we find between inner and outer leaflet membrane mixing (Figure 2) and between transient pores and the formation of fusion pores (Figure 3). This lag period in biomembrane fusion has been variously interpreted. In one widely held view (Lindau & Almers, 1995; Blumenthal *et al.*, 1996), the initial transient pore is "surrounded by a ring of protein, and it expands by breaking the ring and recruiting lipid into its circumference" (Lindau & Almers, 1995); the evolution of a proteinaceous pore to a lipidic pore accounts for the delay time. In another view (Zimmerberg *et al.*, 1991), the initial flickering pore consists of a "hydrated lipid-lined protein pore" complex that widens until the fusion proteins dissociate from the complex and the pore becomes irreversible; the time required to recruit additional protein−lipid complexes accounts for the delay. A variation of this model suggests "that larger pores are formed from a series of smaller [transient] pores" (the sieve model; Zimmerberg *et al*, 1994). In yet a third view (Monck & Fernandez, 1992; Monck *et al.*, 1995), the initial flickering pore is seen as reflecting a fluctuating lipidic junction between two stressed and closely apposed lipid bilayers held in place by a "protein scaffold". In this view, initial lipidic pores "fluctuate around a certain size before either expanding irreversibly or closing". Presumably, this would account for the delay time. In our studies, the observed delay reflects the "maturation" of an unstable, reversible lipidic intermediate (I_1) to a fusion-committed intermediate (I_2) that persists even in the absence of aggregating concentrations of PEG.

The remarkable parallels between PEG-mediated SUV fusion and biomembrane fusion suggest that the electrophysiological events observed during cell membrane fusion might be accounted for in terms of structural rearrangements between closely contacting, stressed lipid bilayers. Thus, the pores that form during biomembrane fusion may well be lipidic in nature, as suggested by Monck and Fernandez (1992), and not proteinaceous in nature, as proposed by Lindau and Almers (1995) or Zimmerberg *et al.* (1991). In this view, proteins would serve to direct appropriate membranes to each other, bring their bilayers into close contact, destabilize contacting bilayers so the initial, unstable lipidic pore (I_1) structure can form, and then maintain this intermediate until it can mature into a semistable lipidic intermediate structure (I_2) that spontaneously and irreversibly disintegrates to create a fusion pore. In this view, protein machines organize, direct, and drive fusion, but in doing so, they must deal with the physical properties of the essential structural element of a biomembrane, the lipid bilayer. The results presented here demonstrate that PEG-mediated vesicle fusion may provide a powerful model for revealing the structural details of the biomembrane fusion process.

REFERENCES

Arnold, K., Zschoernig, O., Bacthel, D., & Herold, W. (1990) *Biochim. Biophys. Acta 1022*, 303−310.

Blumenthal, R., Sarkar, D. P., Durell, S., Howard, D. E., & Morris, S. J. (1996) *J. Cell Biol. 135*, 63−71.

Brekenridge, L. J., & Almers, W. (1987) *Proc. Natl. Acad. Sci. U.S.A. 84*, 1945−1949.

Burgess, S. W., & Lentz, B. R. (1993) *Methods Enzymol. 220*, 42−50.

Burgess, S. W., Massenburg, D., Yates, J., & Lentz, B. R. (1991a) *Biochemistry 30*, 4193−4200.

Burgess, S. W., Wu, J. R., Swift, K., & Lentz, B. R. (1991b) *J. Fluoresc. 1*, 105−112.
Burgess, S. W., McIntosh, T. J., & Lentz, B. R. (1992) *Biochemistry 31*, 2653−2661.
Chen, P. S., Jr., Toribara, T. Y., & Warmer, H. (1956) *Anal. Chem. 28*, 1756−1758.
Chernomordik, L., Chanturiya, A., Green, J., & Zimmerberg, J. (1995) *Biophys. J. 69*, 922−929.
Chernomordik, L. V., Melikyan, G., & Chizmadzhev, Y. A. (1987) *Biochim. Biophys. Acta 906*, 309−352.
Chizmadzhev, Y. A., Cohen, F. S., Shcherbakov, A., & Zimmerberg, J. (1995) *Biophys. J. 69*, 2489−2500.
Clement, N. R., & Gould, J. M. (1981) *Biochemistry 20*, 1534−1538.
Ellens, H., Bentz, J., & Szoka, F. C. (1986) *Biochemistry 25*, 285−294.
Fernandez, J. M., Neher, E., & Gomperts, B. D. (1984) *Nature 312*, 453−455.
Hoekstra, D., de Boer, T., & Wilschut, J. (1984) *Biochemistry 23*, 5675−5681.
Kemble, G. W., Danieli, T., & White, J. M. (1994) *Cell 76*, 383−391.
Kozlov, M. M., Leikin, S. L., Chernomordik, L. V., Markin, V. S., & Chizmedzhev, Y. A. (1989) *Eur. Biophys. J. 17*, 121−129.
Lakowicz, J. R. (1983) *Principles of Fluorescence Spectroscopy*, Plenum Press, New York.
Lee, J., & Lentz, B. R. (1997) *Biochemistry 36*, 421−431.
Lentz, B. R., & Burgess, S. W. (1989) *Biophys. J. 56*, 723−733.
Lentz, B. R., Carpenter, T. J., & Alford, D. R. (1987) *Biochemistry 26*, 5389−5397.
Lentz, B. R., McIntyre, G. F., Parks, D. J., Yates, J. C., & Massenburg, D. (1992) *Biochemistry 31*, 2643−2653.
Lentz, B. R., Talbot, W. A., Lee, J., & Zheng, L.-X. (1997) *Biochemistry 36*, 2076−2083.
Lindau, M., & Almers, W. (1995) *Curr. Opin. in Cell Biol. 7*, 509−517.
Massenburg, D., & Lentz, B. R. (1993) *Biochemistry 32*, 9172−9180.
McIntyre, J. C., & Sleight, R. G. (1991) *Biochemistry 30*, 11819−11827.
Meers, P., Mealy, T., Pavlotsky, N., & Tauber, A. I. (1992) *Biochemistry 31*, 6372−6382.
Meers, P., Janoff, A., & Ali, S. (1996) *Biophys. J. 70*, A83.
Melikyan, G. B., White, J. M., & Cohen, F. S. (1995) *J. Cell Biol. 131*, 679−691.
Monck, J. R., & Fernandez, J. M. (1992) *J. Cell Biol. 119*, 1395−1404.
Monck, J. R., Oberhauser, A. F., & Fernandez, J. M. (1995) *Mol. Membr. Biol. 12*, 800−809.
Oberhauser, A. F., Monck, J. R., & Fernandez, J. M. (1992) *Biophys. J. 61*, 800−809.
Paula, S., Volkov, A. G., Van Hoek, A. N., Haines, T. H., & Deamer, D. W. (1996) *Biophys. J. 70*, 339−348.
Perin, M. S., & MacDonald, R. C. (1989) *J. Membr. Biol. 109*, 221−232.
Spruce, A. E., Breckenridge, L. J., Lee, A. K., & Almers, W. (1990) *Neuron 4*, 643−654.
Spruce, A. E., Iwata, A., & Almers, W. (1991) *Proc. Natl. Acad. Sci. U.S.A. 88*, 3623−3627.
Suurkuusk, J., Lentz, B. R., Barenholtz, R. L., Biltonen, R. L., & Thompson, T. E. (1976) *Biochemistry 15*, 1393−1401.
Talbot, W. A., Zheng, L.-X., & Lentz, B. R. (1997) *Biochemistry* (in press).
Tse, F. W., Iwata, A., & Almers, W. (1993) *J. Cell Biol. 121*, 543−552.
Viguera, A. R., Mencia, M., & Goni, F. M. (1993) *Biochemistry 32*, 3708−3713.
Wilschut, J., Düzgüneş, N., Fraley, R., & Papahadjopoulos, D. (1980) *Biochemistry 19*, 6011−6021.
Wilshut, J., & Hoekstra, D. (1986) *Chem. Phys. Lipids 40*, 145−166.
Wu, H., Zheng, L.-X., & Lentz, B. R. (1996) *Biochemistry 35*, 12602−12611.
Wu, J. R., & Lentz, B. R. (1991) *Biochemistry 30*, 6780−6787.
Wu, J. R., & Lentz, B. R. (1994) *J. Fluoresc. 4*, 153−163.
Zimmerberg, J., Curran, M., & Cohen, F. C. (1991) *Anal. N.Y. Acad. Sci. 635*, 307−317.
Zimmerberg, J., Blumenthal, R., Sarkar, D. P., Curran, M., & Morris, S. J. (1994) *J. Cell Biol. 127*, 1885−1894.

BI970404C